Zero Degree Calorimeters for RHIC

QCAL Group:

Brookhaven, Frankfurt, IHEP (Protcvino), Maryland, TAMU

April 10, 1998

Abstract

Two mechanisms for forward, correlated neutron emission in heavy ion collisions motivate the construction of compact hadron calorimeters to be placed downstream of interaction regions at RHIC and LHC. Plans are now underway to build such detectors. Here we discuss recent progress in understanding their role and performance requirements.

1 Introduction

Zero **D**egree **C**alorimeters (ZDC's) are now being built for the RHIC heavy ion experiments. They will subtend an angle of $\sim$ 2.5 mr about the forward direction on each side of the interaction regions.

The calorimeters are designed to measure beam energy neutrons emitted in the breakup of the nuclear remnant that misses the interaction zone (so-called "spectator fragment"). The usefulness of this measurement was evaluated in a test carried out at the CERN SPS.

Since the neutrons have a soft emission spectrum and therefore limited transverse spread ($P_t \sim 100$ MeV) , their energy is fully contained in the ZDC's.

The calorimeters will also be the principle device used for luminosity monitoring during heavy ion runs. The inclusive correlated emission of neutrons in each beam direction corresponds to a large cross section, calculable with small uncertainty.

In this report we present in outline the cross section calculation and describe the experimental measurement of neutron multiplicity vs. impact parameter.

A tungsten/Cerenkov fiber sandwich calorimeter design was developed and prototyped for this project and evaluated in a high energy proton beam at the CERN SPS. Initial results on performance of this device are presented. Finally we describe the plan for construction Installation and Running of the detectors.

2 Role of the calorimeters

In Heavy Ion collisions, the collision impact parameter is, in principle, a measurable and useful quantity. In the search for new states of matter under conditions of extreme density and temperature it will be useful to characterize collisions using global measurements which don't bias the signal of interest.

In order to compare results from different experiments we also seek measurements of global event properties which use common instrumentation.

In fixed target experiments at the AGS and CERN SPS, Global event properties corresponding roughly to impact parameter were measured using central multiplicity, Et and the complementary energy flow from the noninteracting ion remnants which remain undeflected in the beam downstream of the collision. As expected, large central energy (E_t) was strongly anti correlated with the forward "zero degree" energy.

2.1 Event Characterization with a neutron Calorimeter

At RHIC we will measure only the zero degree energy that is emitted as neutrons since the forward direction can be accessed only downstream of the magnets that separate stored beams at each interaction point. Charged fragments will be deflected along with the stored beam. In order to confirm the effectiveness of the zero degree neutral energy measurement at future colliders (RHIC and LHC) a special test of this restricted measurement was carried out within the NA49 experimental setup at CERN. By applying a magnetic field to the region downstream of the interaction target we were able to separately measure the degree of correlation between Et (or equivalently impact parameter) and the zero degree energy in the form of neutrons as opposed to the total zero degree energy.

In the NA49 run [5], "centrality" of 158 GeV/n Pb + Pb target collisions was measured simultaneously using a large angle "ring" calorimeter and a forward (ZDC) calorimeter, $\sim$ 25 m downstream of the target. A magnet between the target and ZDC separated the fragments so that different species could be measured independently. The resulting geometry, shown in Fig. 1, is identical to the configuration around the RHIC neutron detector location. The "fragment" region corresponds to the orbit of one stored beam.

The results of this test [5] demonstrate a strong correlation between neutron energy and impact parameter. It was also found that the average number of spectator neutrons is large and varies from $\sim$ 8 neutrons at 0 impact parameter to $\sim$ 30 neutrons at intermediate impact parameters. In other words, central (Au- Au or Pb-Pb) collisions are always accompanied by beam energy neutrons in both beam directions.

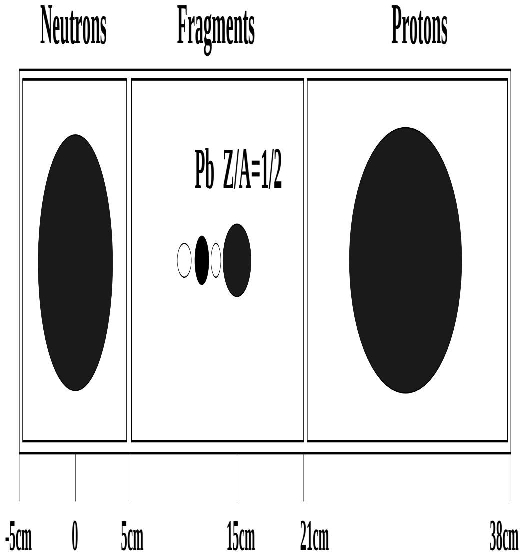

Figure 1: Fragment distribution at the forward calorimeter in the NA49 test.

2.2 Mutual Coulomb Dissociation and Luminosity Monitoring

The Coulomb dissociation of a single beam nucleus in collisions of identical beam species has already been considered in some detail for RHIC [4],[3]. This process is of interest because it is one of the limiting factors affecting beam lifetime. However, we do not consider it interesting as a diagnostic tool since it is not easily distinguished from "single beam" backgrounds. On the other hand, we find that a simple extension of the Weizsacker-Williams treatment for this process reveals a large component of mutual dissociation [1]. The coincident detection of neutrons along each beam direction makes the process cleaner and suitable for **luminosity monitoring**.

The cross section for heavy ion dissociation may be accurately expressed in terms of the (experimentally known) photo dissociation cross sections, $\sigma_{ph}(\omega)$, of the same nucleus over an appropriate range of photon energies.

$$\sigma_{dis} = \frac{2\alpha Z_p^2}{\pi\gamma^2} \int d\omega\omega\sigma_{ph}(\omega) \int_{b_0}^{\infty} b\, db K_1^2(\frac{b\,\omega}{\gamma}). \tag{1}$$

Since we want to calculate the mutual dissociation cross section for the two colliding nuclei, we define a dissociation probability, P(b), as a function of impact parameter b

$$\sigma_{dis} = 2\pi \int_{b_0}^{\infty} P(b) b \; db. \tag{2}$$

Then inverting the order of integration in Eq. (1) we have

$$P(b) = \frac{\alpha Z_p^2}{\pi^2 \gamma^2} \int d\omega \omega \sigma_{ph}(\omega) K_1^2 (\frac{b\,\omega}{\gamma}). \tag{3}$$

We neglect, for the moment, the fact that P(b) approaches unity at grazing impact in our case. We instead give a first order expression for correlated dissociation, $\sigma_{cd}^{(1)}$, which we subsequently correct to preserve unitarity. We then have

$$\sigma_{cd}^{(1)} = 2\pi \int_{b_0}^{\infty} \Big[P(b) \Big]^2 b \; db, \tag{4}$$

which may be evaluated numerically using the data on $\sigma_{ph}(\omega)$. As discussed in ref. [1], the resulting cross sections are sensitive to impact parameter cutoff (b_0) at the level of 10 to 15%. Taking $b_0 = 15$ fm, we found σ_{cd} =3.9 barns at RHIC top energy with gold beams and 7.2 barns at LHC top energy with Pb beams.

The sensitivity to impact parameter cutoff can be essentially eliminated [2] if we sum over both Coulomb and Nuclear contributions to the correlated neutron emission cross section. This simplifies the picture both experimentally and theoretically. Theoretically, the picture is simpler because once Heavy Ions overlap, the neutron emission probability due to nuclear interactions saturates. This finesses the issue of minimum impact parameter for the Coulomb calculation. Experimentally the picture is simpler because we need only measure the coincidence rate of neutrons in each beam direction.

3 Experimental Considerations, Detector Requirements

The spectrum of emitted neutrons determines the design criteria for the luminosity monitor detectors. Their lab energy and angular distributions were calculated from photo nuclear data. More than half of the inclusive dissociation cross section results in single neutron emission with a lab energy spread of $\sigma \leq 10\% \times E_{beam}$. So the measured line width will be determined by the detector resolution which we therefore require to be $\leq 20\%$ at 100 GeV.

The angular distribution is limited to a cone of 1.4 mr opening angle at RHIC top energy (± 2.5 cm at the ± 18 m location of the detectors in RHIC). The neutron calorimeter response should be flat over this area. The final requirement on the 2 calorimeters comes from the possibility to locate the interaction point from time difference measurement. We require $\sigma_t \leq 300$ psec.

4 Calorimeter Design

4.1 ZDC Geometry

The zero degree calorimeters will be located along what is referred to as zero degree line of the RHIC. There will be two calorimeters for each of the four RHIC experiments, they will be set to the left and to the right of the interaction region (*ir*). The beam geometry and detector location are illustrated in Fig. 2.

The interaction point is located at the center of the berilium beampipe. Following flanges and a steel beampipe section the DX magnet is located approximately at 11.65 m on either side of the *ir*. For reference, the DX magnets are warm bore, super conducting dipole magnets, the total length of the DX magnet assembly, from flange to flange, is $\sim$ 6.11 m. The downstream end of the DX magnet is approximately 14.73 m from the interaction point. Following the DX magnet there is a bellows section of pipe with a diameter of $\sim$ 30.5 cm, and a length of $\sim$ 50 cm. In the present design this bellows is followed by a conical pipe. The diameter of this pipe starts at $\sim$ 30.54 cm on the end that attaches to the bellows, and increases along its length to a final diameter of 41.9 cm. The length of this conical pipe is $\sim$ 267 cm. The downstream end of this pipe is closed off with a plate that contains two 12.7 cm diameter holes, centered horizontally, with a distance of 24.51 cm between the centers of the holes. Individual 12.7 cm diameter beam pipes carry the incoming and outgoing beams from this point to flanges $\sim$ 1.7 m further downstream from the *ir*.

The maximum possible distance between beampipes consistent with different machine operating configurations was calculated in RHIC Det. Note # 6 [12] and found to be 15 cm at the downstream end of the warm section. The distance between two beam pipes that attach to the plate at the end of the conical pipe is 11.81 cm in the current RHIC design (a revised figure of this region is in preparation). The angle that these pipes make with respect to the zero degree line is + and - about 18.7 mrad. The total distance from the interaction region (*ir*) to the downstream face of the plate, at the end of the conical tube, is of about 17.85 m.

About 40 cm further downstream from the plate at the end of the conical pipe, one gets to a point where the total distance between the two pipes is about 13.31 cm. It is at this point, approximately 18.25 m downstream from the interaction point, where the zero degree calorimeters will be placed allowing 1.66 cm for clearance on each side. The calorimeter will be placed then between the two beam pipes that extend downstream for 1.7 m before encountering a flange. The distance between the two flanges at this point is 17.2 cm. About 30 cm past the start of these flanges one reaches a gate valve on each pipe. There is essentially no space between these gate valves, so this defines the maximum distance from the IP for a zero degree detector to end.

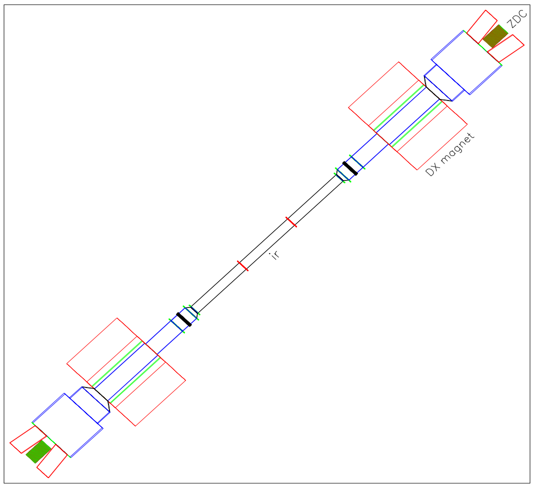

Figure 2: ZDC geometry.

4.2 Simulations

The design choice is based on the simulation of performance of options fitting within the available transverse dimensions.

Unless otherwise specified, all cases are for Cerenkov fiber sampling with a 45^o tilt angle of absorber and fiber with respect to the beam direction. The reasons for this choice are given elsewhere [12]. The options were scoped by simulating with Geant the response to neutrons distributed over the front face of the calorimeter with a p_t distribution characterized by Fermi motion. In fact the p_t distribution for Mutual Coulomb Dissociation will be somewhat narrower and transverse leakage effects should be less severe.

Most of the ZDC special requirements are in, fiber numerical aperture(NA) and orientation, and photoelectron response for visible and for uv, and three readout devices, quartz and borosilicate glass pmts and HPDs. The code has been checked on all of the experimental ZDC data for EM and Hadronic response listed in the references below.

The results for absorber choice with our geometrical restrictions in order are: uranium, tungsten, tantalum, lead and copper is last. All are viable, but lead and copper cannot make the energy resolution target of 20% at 100 GeV. The factors considered, in rough order of deterioration of the energy resolution(or at least ease of doing something about it) are:

1. shower leakage, mainly transverse due to the 10cm dimension
2. intrinsic binding energy fluctuations, mainly pi-zero fluctuations
3. sampling fluctuations
4. photon statistics

4.3 Shower Leakage

Use of uranium or tungsten brings the shower Cerenkov-sensitive shower leakage under control and switches the priorities (1) and (2) above. It is near the top because it costs money. Use of the dense absorbers also makes a more compact structure longitudinally and it is more certain that a 8 λ structure will fit in the final RHIC design. Uranium is best for energy resolution because of a smaller e/mip and thus a better e/h ratio as described later. Uranium may be a bit cheaper than tungsten, even with $300/hr machine shop time, but we almost certainly cannot use it because of environmental reasons.

The short attenuation length of tungsten helps the transverse containment, but the situation is a little more complicated and hurts the usefulness of copper more than expected. The fiber numerical aperture is important (the whole method depends on it) so NA=0.22 is needed here. But it must be must remember that the shower dimension shrinkage over dE/dX devices is 1/2 to 1/3, at the 80-90 % containment radii, and still is in conflict with the 10 cm dimension.

Table 4.3 shows results of our calculations (which whenever possible have been compared to data [7]) . Copper is apparently slightly worse than lead. Except where noted, the results are for 100 GeV protons, 200 micron NA = 0.22 quartz fiber, uv +vis light XP2020Q pmts and the 45 degree tilted plates.

Table 1: Results for likage calculations.

absorber	thick(cm)	r(90%) cm	leak
CU	1.4	7.87	26
Cu	1.0	7.93	27
W	0.35	4.59	8
Pb	0.56	7.91	26
U	0.32	4.92	9
Cu	1.0	8.75	30

The energy resolution can be calculated as given in Table 2 with various components contributing to this resolution [9]. The sigma values are given separately except for leakage which is integrated with sampling and photoelect. statistics. The resolution scales with 1/SQRT(E) to this point, with little constant term. Binding energy fluctuations may need more work and may be underestimated somewhat. These are dominated by pi-zero statistics and will not scale as 1/SQRT(E), and are the major source of the constant term in sigma/E.

Table 2: Energy resolution.

abs.	thick (cm)	sig samp	sig pe	sig s+pe+leak	e/h sig	BE	sig-total e-res
Cu	1.4	7.0%	9.8%	24%	5.3	17.6%	29.8%
Cu	1.0	5.8	7.5	19.3	5.2	17.7	27.4
W	0.35	4.6	5.6	9.7	2.9	14.4	17.3
Pb	0.56	4.4	7.4	17.5	2.5	13.6	22.2
U	0.32	4.2	5.5	9.4	2.1	12.6	15.7
W*	1.0			8.5	1.0	2.5	8.9

W* is a tungsten- liquid scintillator design, included for perspective The resolution for lead would be worse because an 8 λ structure would not fit. Most plate thicknesses are 1X, except for Cu, where it makes no difference i.e. the 1.0 cm has no effect on e/h.

The 0 degree fiber e/h intrinsic ratio value for Cu is 7.3, in good agreement with estimates given in Wigman's 1995 NIM paper [8]. The e/h ratios for Pb are 3.5 for 0 deg. fibers and 2.5 for 45 degrees as given in the table. These disagree with fits to simulated data in ref. [10, 11].

Having selected Tungsten as an optimal choice for absorber material it is possible to modify the plate thickness and fiber thickness in order to select among ready options for plates which are available "off the shelf". It was proposed to work with 2.5 mm plates. The results are shown in Table 3.

Table 3: Absorber material.

entry	thick(mm)	s. res	pe res	s+pe+leak	e/h	BE res	total
1	3.5	4.6	5.7	9.7	2.9	14.4	17.3
2	5.0	5.5	5.7	10.5	2.8	14.3	17.8
3	5.0	5.5	4.8	9.6	2.8	14.3	17.2
4	2.5	3.9	4.8	9.2	3.8	18.1	20.2

The first entry should be identical to the previous 3.5 mm W, 200 micron fiber 10 cm dimension and 8 λ deep. The second entry only increases the plate thickness to 5.0 mm and the third entry also increases the fiber to 400 micron. The fourth entry uses 2.5 mm tungsten and 200 micron fiber.

Entry 1 has 155 layers, entries 2,3 109 layers, entry 4 has 217 layers. If anything, the binding energy term is underestimated . The bonding of two 2.5 mm plates with a radiation resistant agent is our choice for the design given below.

One sees that the intrinsic fluctuations dominate, and that is the reason to to try to reduce the plates, i.e. reduce e/h.

4.4 Fiber Choice

The original simulations assumes the use of a Cerenkov fiber with a small numerical aperture (NA = 0.22). These fibers are available commercially with Quartz core. However, for the RHIC application a dose over a 10 year period is expected to be in the few 10^4 range. Thus this was not the main argument for using or not the quartz fiber. Quartz fiber is generally more expensive and more difficult to polish and handle.

Instead of Quartz fiber, plastic fiber could be used. It appeared feasible to make low index PMMA core/PMMA clad fiber, however it has not been found yet a commercial source for this fiber. It is not known if low NA polystyrene core fiber is available. The PMMA fiber is just marginally acceptable for our application, having typical induced attenuation of ≤ 1 dB/m at doses of 10^4 rads. Finally, the PS fiber is another feasible choice since it is more radiation hard than the PMMA fiber by at least an order of magnitude in the 400 nm to 500 nm wavelength region [14].

The pricing assumption is 50 cents/meter for 0.5 mm diameter fiber, provided the continuation of the search for vendor quotes for fiber with a low numerical aperture. The assumed photostatistics with the fiber and photodetector combination is based on lab tests with cosmic muons. It was found a yield of 0.5 photoelectrons per mm.

4.5 Calorimeter Design Summary

Installation of Zero Degree Calorimeters at RHIC is made possible by the existence of a warm beamtube section between the magnetic elements in the machine which steer beams from the two rings into head-on collisions at each interaction region. The beam geometry and the detector locations are illustrated in Fig. 2.

The available space is limited laterally by the space between the beamtubes to ~ 12 cm. A major consideration in the design of the ZDC's is therefore that they be compact and exhibit a minimum non-uniformity of response near the detector edges. Since simulations and beamtests have demonstrated that a cerenkov rather than scintillator sampling calorimeter has a narrower response to hadronic showers [10] we chose a design with alternating absorber and Cerenkov fiber layers. The fibers (PMMA for the prototypes and early running at RHIC and more radiation hard silica fibers for later stages of RHIC running) are formed into layers (ribbons) in which Cerenkov radiation is produced and channeled to a PMT when traversed by shower particles within a limited angular cone.

We chose a design with fiber layers oriented at 45^o to the beam direction [6] because this orientation leads to the highest light yield and the best discrimination against background particles entering from the back of the calorimeter.

Our simulations showed that a hadronic shower resolution of $\leq 20\%$ at 100 GeV can be achieved with a 10 cm wide by 8 λ deep module with 5mm thick Tungsten sampling layers.

We also tested performance with a 6 λ prototype and obtained essentially identical results. The 6 λ design has since been selected for our project. Finally, an inexpensive Copper version of the calorimeter was also built and tested but we do not report those results here.

5 Prototype Test

We tested the prototype modules in the fall '97 proton run at CERN. The test was performed during the month of November as part of the NA49 run. For calibration purposes, a small muon component present in the beam was selected for part of the data.

5.1 Testbeam Results

The design of the prototype modules is illustrated in Fig. 3. The modules (each 2 nuclear interaction lengths long) were placed on a movable stage just upstream of the NA49 ring calorimeter. The modules were read out with 2 " Hammamatsu PMT's (R-329-02) and their anode signals were run over 45 ft of (rg-58) coaxial to a passive splitter which divided the signal equally between a leading edge discriminator and an LRS 2249a ADC. The discriminator output was used to record time of flight in a 50 psec resolution CAMAC TDC.

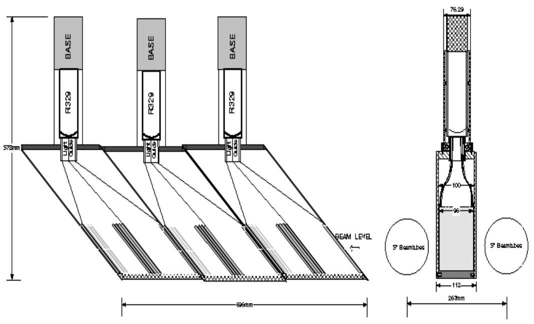

Figure 3: ZDC Design.

For the purposes of this run, beam Muons were used to obtain relative calibration of the calorimeter depth segments. Phototube gains were adjusted so that muon peaks in all modules appeared in the same adc channel.

Also a measure of the photoelectron yield of each module was performed by using line shape and assumed Poisson statistics. Tests on fiber ribbons prior to building the calorimeter gave 0.7 $p.e./mm$ of fiber thickness. Initial tests with cosmic muons at BNL also gave in the range of roughly 12 $p.e/module$. Since one module has 27 0.5 mm thick fiber layers these results are reasonably consistent.

Measurements at CERN with muons in the testbeam gave approximately 16 $pe/module$. Since the energy loss in one module is estimated to be of order 7.5 GeV it is clear that photostatistics have a negligible contribution to the module energy resolution at 100 GeV.

In this exercise all modules were gain balanced using the μ peaks. Calibration energy thus has no free parameters relating the weight of depth segments.

An led flasher system was also installed. During RHIC operation we plan to use the flasher system to monitor gain. However in the NA49 test, muon runs were available so frequently that there was no need to also take low rate flasher data.

5.1.1 Energy Linearity of the Calorimeter

Having preset the gains, data were taken with 100 and 160 GeV protons. The gaussian fits to the pulse height distributions shown in Fig. 4 at the 2 energies yield $616/380 = 1.62$ in excellent agreement with linear response

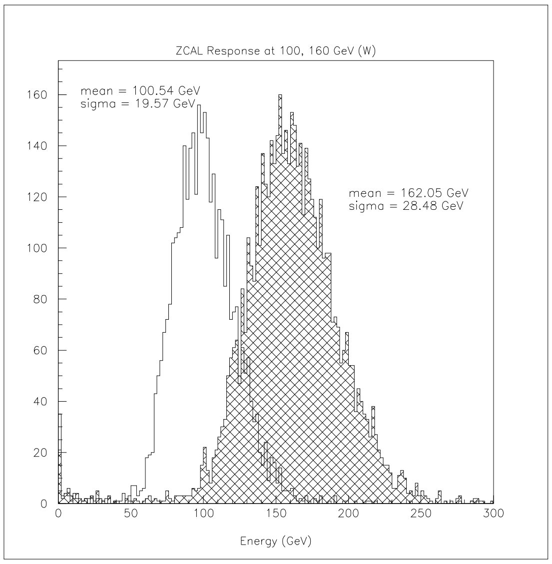

Figure 4: Energy Linearity, Tungsten Calorimeter.

From a fit the resolution (rms of gaussian fit) vs energy, there is evidence for a significant constant term -of order 10 %. This is about the level that was found in CMS tests with copper modules with varying sampling frequency.

5.1.2 Response map of the calorimeter

Figures 5 and 6 show variation of amplitude and sigma over the face of the detector. Also displayed is the response obtained with only 3 modules (6 lambda) and for the flipped calorimeter (where the beam was actually incident from the back of the detector). The scanning was done both along horizontal (X) and vertical (Y) axes, of the calorimeter.

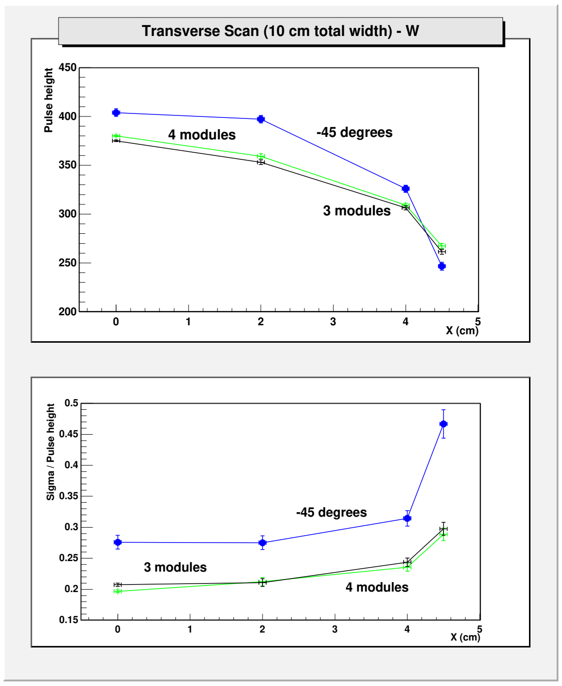

Figure 5: Horizontal scanning, Tungsten calorimeter.

5.1.3 Timing resolution

The time measurement of the calorimeter modules was corrected for pulse height slewing off-line.

Using the time difference distributions between modules 1 and 2 and from time distributions relative to a beam counter we find that module 1 (the first 2λ) gives the best timing resolution and obtain $\sigma_t \leq 230$ psec. Fig .7 shows the resolution of the time difference between the first module relative to the beam counter.

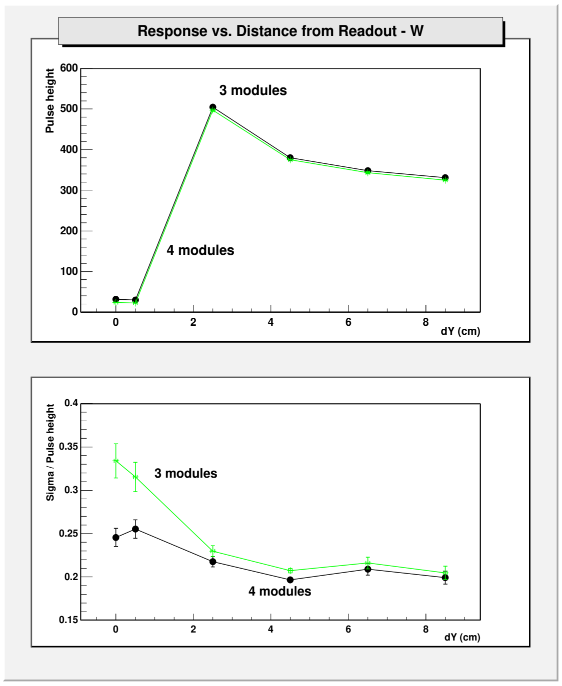

Figure 6: Vertical scanning, Tungsten calorimeter.

Based on this time resolution we calculate that the interaction point in a typical event can be determined to of order 2 cms.

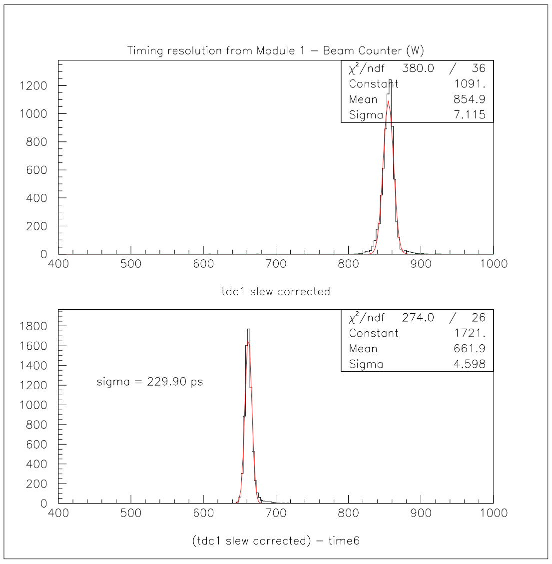

Figure 7: Timing, Module 1 and beam counter (6).

6 Plan for Construction, Installation and Running in

The Basic Scope of the ZDC project is summarized in the following sections

- Group Responsibilities
- Schedule Table
- Construction Budget Table

Following the successful prototype tests at CERN and the collaboration meeting at BNL in February 1998, we have decided to proceed with a final design for the calorimeter based roughly on the 6λ Tungsten design tested at CERN. The major change is an increase in vertical size by 25% to reduce the effects of shower leakage near the readout end.

The completion of the design and construction of the production prototype will take place at Frankfurt by the end of April with close coordination of Texas AMU and IHEP who are responsible for fabrication of absorber plates and fiber ribbons respectively.

We are committed to installing as many zdc's as there are experiments ready to commission them by June 1, 1999 and plan to install at least 1 set of "sacrificial" ZDC's (probably just on one side of an interaction region) in time for the first stored beams in RHIC in Spring '99.

In the long term we look to the eventual dose of $\sim$ 100 Gy radiation dose in RHIC [13] as a likely source of radiation damage. We are planning to carefully instrument the region around at least one set of ZDC's to track actual absorbed dose and will consider measures to reduce the radiation damage (increased attenuation) to the PMMA fibers- such as maintaining them in an N2 atmosphere.

In the meantime IHEP is developing a design and evaluation for radiation hard silica fibers. A decision on when to replace quartz fibers will be made some time during 1999 based on results of dose measurements.

6.1 Group Responsibilities

The group responsibilities, the institution and the responsible physicist are showed in Table 4.

Commission ZDC's at RHIC (i.e. tune HV, Calibrate and Provide Coincidence signals) are responsibility of the **individual experiments**, the contacts are:

STAR	W. Christie
BRAHAMS	M. Murray
PHOBOS	E. Garcia
PHENIX	S. White

6.2 Schedule Table

Table 5 shows the proposed time for the project and lists which institute is responsible for each item.

6.3 Construction Budget Table

Table 6 shows the costs of constructing the calorimeters. The total cost is about \$201k. This does not include the cost to the individual experiments and the RHIC controls group, of using the calorimeters.

Table 4: Group responsibilities table

Task	Institution	Responsible Physicist
Design of Assembly, Drawing Control, Lift Fixtures, Documentation	Frankfurt	H.Strobele
Design and Purchase of Tungsten Absorber Plates	TAMU	M.Murray
Purchase of PMMA 0.5 mm diameter fibers, Ship to IHEP	Frankfurt	C.Adler
Prepare Fiber Ribbons, Liaison with Frankfurt on Design aspects for ribbon Installation	IHEP	A.Denisov
Construct 18 zdc modules (sufficient for 3 Expts.), perform QA on average photoelectron yield, document and ship to BNL	Frankfurt	H.Strobele
Construct remaining 6 zdc modules, QA, etc.	TAMU	M.Murray
Design and Build Stands for the ZDC Modules which may also support shielding and muon trigger counters	BNL	W.Christie
Prepare PMT's and Bases and Screen PMT's	BNL & UMD	E.Garcia
Prepare Cosmic Ray test stand, rad monitoring devices for RHIC, muon trigger	BNL & IHEP & UMD	S. White
RHIC Interface, Slow Controls, Scaler readout	BNL	A.Drees
Develop Rad Hard Version 4 of fiber Ribbons	IHEP	A.Denisov

Table 5: Timeline for construction of Zero Degree Calorimeters. On January 4th 1999 the first beams should be circulating in the RHIC ring. Colliding Beams are expected in mid 1999.

Date	Task	Institute
9 Feb 98	Start Design	F.U. & TAMU
5 Mar 98	Finish plate design	F.U. & TAMU
10 Mar 98	Start procurement of W plates	TAMU
15 Mar 98	Start getting Fiber bids	BNL & F.U.
15 Mar 98	Test existing PMT tubes	M.U.
24 Mar 98	Begin design of stand	BNL
24 Mar 98	Full Design of modules	F.U. & TAMU
1 Apr 98	Final choice PMT at F.U.	M.U. & BNL
5 Apr 98	1st fiber ribbons delivered to F.U.	IHEP
15 Apr 98	Start assembly of "Aluminum" module	F.U. & TAMU
1 May 98	Aluminum module assembled with fibers	F.U. &
		TAMU & IHEP
1 May 98	Place W order for "rest" (or all) of plates	TAMU
1 May 98	Finalize Fiber ribbon design	F.U.&
		TAMU & IHEP
1 May 98	Specify H.V. and RHIC control	
	crate placement	**Exps.** & BNL
1 Jul 98	Order PM tubes	BNL
1 Aug 98	Deliver all fiber ribbons to TAMU & F.U	IHEP
1 Sep 98	Take Delivery of W plates	
	assembly of modules	
	(6 weeks @ 3 modulesweek)	F.U. & TAMU
1 Oct 98	Install at least 4 stands in ring	BNL
1 Oct 98	Delivery of PM tubes	BNL
20 Oct 98	Ship Modules to BNL	F.U. & TAMU
1 Nov 98	Attach PMTs and begin test & calibration	BNL & UMD
15 Dec 98	Install one assembly (3 modules) in ring	BNL & UMD
4 Jan 99	Begin commissioning	BNL

Table 6: Costs of constructing the calorimeters

Item	Cost	Remarks
Tungsten	$ 53.9k	
PMMA Fiber	$ 4.8k	
Plate Assembly & Support	$2k	Frankfurt
	$5k	TAMU
PMT Mounts	$12k	Frankfurt
Manufacture Stands	$8k	
PMT's and Bases	$12k	R-329 or equiv
LED Flasher Hardware	$8k	
Making Fiber Ribbons	$10k	27/module, 650 total
R&D for quartz fibers	$5k	
Quartz Fiber	$80k	
Total	$200.7K	

References

[1] A. J. Baltz and S.N.White, BNL-63127.

[2] A. J. Baltz, C.Chasman and S.N.White, submitted to Nucl. Instr. and Meth.

[3] M. J. Rhoades-Brown and J. Weneser, BNL-47806.

[4] A. J. Baltz, M. J. Rhoades-Brown, and J. Weneser, BNL-63069.

[5] T.Alber et al.(na49 collaboration) manuscript in preparation.

[6] M.Lundin et al., Nucl. Inst. and Meth. A 361 (1995) p.161

[7] Quartz Fibre Calorimetry-Monte Carlo Simulation, G.Anzivino et al. NIM A357 (1995) 380-385

[8] Quartz Fibre Calorimetry for LHC experiments, O.Ganel and R. Wigmans NIM A 365(1995) 104-116

[9] On the electromagnetic Energy Resolution of Cherenkov-Fiber Calorimeters M.Lundin et al. NIM A 372(1996)359-367

[10] Quartz Fiber Calorimetry, P.Gorodetzky et al. NIM A 361 (1995) 161-179 (Copper Simulation)

[11] Recent Developments in Quartz Fiber Calorimetry, G. Anzivino NIM A 357 (1995) 369-379

[12] RHIC Det. Note # 6 A. Drees, Brook Haven National Lab, RHIC.

[13] RHIC Det. Note # 25 Alan J. Stevens, Brook Haven National Lab, RHIC.

[14] J.P.de Brion- Comparative Study of Aging of PMMA and PS optical Fibers. CEN- Saclay report DPHPE 86-07(1986)

[15] Bjorken and McLerran, PRL..

[16] McLerran et al., Frankfurt preprint

[17] Jack Sandweiss, private communication. Some results were presented at RHIC'97 Workshop.